Geophysical Research Letters

RESEARCH LETTER
10.1029/2021GL094941

Strongly Coupled Data Assimilation of Ocean Observations Into an Ocean-Atmosphere Model

Q. Tang[1,2], L. Mu[1,3], H. F. Goessling[1], T. Semmler[1], and L. Nerger[1]

[1]Helmholtz Centre for Polar and Marine Research, Alfred Wegener Institute, Bremerhaven, Germany, [2]Institute of Geographic Sciences and Natural Resources Research, Chinese Academy of Sciences, Beijing, China, [3]Pilot National Laboratory for Marine Science and Technology, Qingdao, China

Key Points:

- Strongly coupled data assimilation is implemented for a coupled ocean atmosphere model
- Satellite sea surface temperatures are the only observations for assimilation
- Strongly coupled data assimilation performs better in the Arctic region than the weakly coupled data assimilation

Supporting Information:

Supporting Information may be found in the online version of this article.

Correspondence to:

L. Nerger,
lars.nerger@awi.de

Citation:

Tang, Q., Mu, L., Goessling, H. F., Semmler, T., & Nerger, L. (2021). Strongly coupled data assimilation of ocean observations into an ocean-atmosphere model. *Geophysical Research Letters*, *48*, e2021GL094941. https://doi.org/10.1029/2021GL094941

Received 10 JUL 2021
Accepted 30 NOV 2021

Author Contributions:

Formal analysis: Q. Tang, H. F. Goessling, T. Semmler, L. Nerger
Investigation: Q. Tang, H. F. Goessling, T. Semmler, L. Nerger
Methodology: L. Nerger
Resources: L. Nerger
Software: Q. Tang, L. Nerger
Supervision: L. Nerger
Validation: Q. Tang, L. Mu, H. F. Goessling, T. Semmler
Visualization: Q. Tang
Writing – original draft: Q. Tang
Writing – review & editing: Q. Tang, L. Mu, H. F. Goessling, T. Semmler, L. Nerger

Abstract We compare strongly coupled data assimilation (SCDA) and weakly coupled data assimilation (WCDA) by analyzing the assimilation effect on the estimation of the ocean and the atmosphere variables. The AWI climate model (AWI-CM-1.1) is coupled with the parallel data assimilation framework (PDAF). Only satellite sea surface temperature data are assimilated. For WCDA, only the ocean variables are directly updated by the assimilation. For SCDA, both the ocean and the atmosphere variables are directly updated by the assimilation. Both WCDA and SCDA improve ocean state and yield similar errors. In the atmosphere, WCDA gives slightly smaller errors for the near-surface temperature and wind velocity than SCDA. In the free atmosphere, SCDA yields smaller errors for the temperature, wind velocity, and specific humidity than WCDA in the Arctic region, while in the tropical region, the errors are generally larger.

Plain Language Summary Satellite sea surface temperature observations are combined with a coupled ocean-atmosphere model to improve the estimation of the ocean as well as the atmosphere variables. This is done by the so-called strongly coupled data assimilation, which updates not only the ocean state but uses the cross-covariance to update the atmosphere variables directly through the assimilation algorithm. The results are compared with the weakly coupled data assimilation, which only updates the ocean state directly. Both of the two assimilation algorithms improve the estimation of the ocean temperature. In the atmosphere, the strongly coupled data assimilation outperforms the weakly coupled data assimilation only in the Arctic region while in the low latitudes the strongly coupled data assimilation deteriorates the results.

1. Introduction

A global climate model represents the physical processes of the ocean, sea ice, atmosphere, and land, as well as their interactions by coupling different components in one system. Within a climate model, the ocean and the atmosphere are the two main compartments, which are highly linked to each other. They give/receive their feedback to/from each other in one system thus influencing each other consistently. In contrast to stand-alone models of the ocean or atmosphere, which rely on forcings, a coupled model essentially evolves freely with little influence of forcings. Therefore, the simulation from a coupled model system may be far away from the real state (e.g., Mulholland et al., 2015). Data assimilation (DA) allows constraining the model state by incorporating observations to correct the model evolution in state space (e.g., Zhang & Moore, 2015). With decent initialization, a coupled system is equipped with the potential for real-world prediction.

There are two main approaches to DA in a coupled system: weakly coupled DA (WCDA) and strongly coupled DA (SCDA) (Penny & Hamill, 2017). WCDA analyses the state of one or more compartments within a coupled system separately by assimilating their own observations and other components in the system are then influenced indirectly via the coupled model dynamics. WCDA is the most commonly used DA approach for a coupled system (Zhang et al., 2020). One example is our previous study (Tang et al., 2020), who assimilated satellite sea surface temperature (SST) and temperature and salinity profiles into the ocean component for a coupled ocean-atmosphere model. The study found improvements of not only the ocean variables, which were directly updated by the DA, but also the atmosphere variables like the air temperature and wind speed. Most of the previous WCDA experiments assimilated observations of both the ocean and the atmosphere (e.g., Browne et al., 2019; Karspeck et al., 2018; Laloyaux et al., 2016), while there are a few studies who assimilated only atmosphere observations (Kunii et al., 2017).

SCDA jointly updates the state of different components within a coupled system through cross-covariances calculated among different components. Observations can be from one or more components. Compared to WCDA, SCDA is able to capture information from different components directly and update them instantaneously by DA instead of only relying on the model dynamics. This is expected to yield more consistent state estimates and better model predictions with a coupled system (Sluka et al., 2016). By now, there are only a few studies focusing on SCDA. Penny et al. (2019) summarized the previous SCDA studies with simplified coupled models like the Lorenz-Stommel model (Tardif et al., 2014) and an idealized single-column atmosphere-ocean coupled model (Smith et al., 2015). A successful example is given by Sluka et al. (2016) who assimilated atmosphere observations to update the ocean and atmosphere variables using a low-resolution general circulation model. Compared to WCDA, they found a reduction of root mean square error (RMSE) up to 60% in both the ocean and the atmosphere, especially for the near surface temperature and sea surface height. However, all of these studies used simplified and idealized models with relatively coarse resolution but no complex climate model with high resolution for a global real-world simulation. Moreover, all previous studies assimilated only the atmosphere observations or both the atmosphere and the ocean observations rather than ocean observations alone. One possible reason is that in a climate model the atmosphere component varies faster than the ocean component. Han et al. (2013) and Zhang et al. (2020) found that SCDA was only effective when the highly accurate, fast varying variables are assimilated, while it is difficult to improve the fast varying component by assimilating observations of the slowly varying component. However, this conclusion was also based on a simplified, idealized coupled system (Lorenz63 coupled to a simple pycnocline ocean model).

Until now, no studies assess the assimilation of ocean observations into both the ocean and atmosphere components with SCDA. This paper analyzes this impact of SCDA with a complex, global ocean-atmosphere model by assimilating real-world ocean observations. Results are compared with WCDA, and ensemble simulations without DA. In summary, this paper investigates: (a) whether SCDA improves the atmosphere state compared to WCDA, and (b) the effect of vertical localization in the atmosphere. The remainder of this paper is divided into four sections. Section 2 introduces the coupled ocean-atmosphere model and the data assimilation method. Section 3 describes the data assimilation experimental settings. Section 4 analyses and discusses the results, while Section 5 provides a brief summary.

2. Model and Data Assimilation Method

2.1. Coupled Ocean-Atmosphere Model

The AWI climate model AWI-CM-1.1 (Rackow et al., 2018; Sidorenko et al., 2015) is a global ocean-atmosphere coupled model. Within AWI-CM-1.1, the sea ice-ocean model FESOM1.4 (Wang et al., 2014) simulates the ocean circulation by solving the primitive equations on an unstructured triangular grid using the finite element method, while the atmosphere model ECHAM6 (Stevens et al., 2013) represents the dynamic atmosphere processes in spherical harmonics and the land surface by the submodel JSBACH. The software OASIS3-MCT (Valcke et al., 2013) serves as the coupler to exchange the air-sea fluxes and surface states.

2.2. Data Assimilation Method

This study performs DA using the local error subspace transform Kalman filter (LESTKF) (Nerger et al., 2012b) for both WCDA and SCDA simulation runs. As one type of ensemble Kalman filter, the LESTKF collects an ensemble of model state realizations to represent the model uncertainties. Here only a short description is given. For a detailed description of the algorithm, we refer to the Supporting Information S1. The state vector can be written as

$$\mathbf{X}_i = \begin{pmatrix} \mathbf{X}_{\text{oce}} \\ \mathbf{X}_{\text{atm}} \end{pmatrix}_i \tag{1}$$

where the subscript i is the realization number, $\mathbf{X}_{\text{oce}}$ is the state vector with ocean variables and $\mathbf{X}_{\text{atm}}$ the vector with atmosphere variables. For WCDA, only $\mathbf{X}_{\text{oce}}$ is included while for SCDA both $\mathbf{X}_{\text{oce}}$ and $\mathbf{X}_{\text{atm}}$ are included. The DA updates the ensemble by combining the observations to correct the model simulations

$$\mathbf{X}^a = \mathbf{X}^f \mathbf{W} \quad (2)$$

at each observation time where the superscripts a and f indicate the analysis and forecast, respectively. $\mathbf{W}$ is the matrix transforming the forecast into the analysis ensemble. Domain and observation localization are used in this study following the method described by Nerger et al. (2012a). No inflation is applied.

2.3. Coupling PDAF With AWI-CM-1.1

The Parallel Data Assimilation Framework (PDAF, http://pdaf.awi.de) (Nerger & Hiller, 2013; Nerger et al., 2005) is an open source software for applying ensemble-based DA. The LESTKF is one of the ensemble-based DA methods implemented within PDAF. PDAF has already been coupled with AWI-CM-1.1 allowing to perform both WCDA and SCDA by assimilating multiple types of ocean observations (Nerger et al., 2020). A seamless sea ice prediction system is further developed by Mu et al. (2020), where different ocean and sea ice observations are assimilated. Tang et al. (2020) used this coupled system to investigate the impact of assimilating different types of ocean observations on the ocean and atmosphere by WCDA.

3. Experimental Settings

The model setup and data assimilation configurations for WCDA are described in Tang et al. (2020) and here, we briefly summarize them.

The horizontal resolution of the unstructured ocean grid varies between 25 and 150 km. The model is discretized into 47 layers in the vertical. The thickness of the top layer is 10 m. Below to surface, the thickness increases linearly to 250 m for the bottom layer. A regular grid is used for the atmosphere, with a horizontal resolution of 1.875° (spectral resolution T63) and 47 sigma-levels. Every hour, the ocean and the atmosphere model exchange fluxes and surface state variables.

DA experiments are performed for the year 2016, using an ensemble of 46 model state realizations. The ocean variables including the sea surface height, temperature, salinity, and velocity in three dimensions are updated daily by DA. A horizontal localization radius of 300 km is used based on tuning experiments minimizing the RMS errors. Daily level-3 satellite SST observations from the E.U. Copernicus Marine Service are assimilated. The original observations have a spatial resolution of 0.1° and are remapped to the unstructured ocean model grid through a data thinning process. An observation error of 0.8°C is applied as in Tang et al. (2020).

To obtain the initial conditions for the DA experiments, first a serial spin-up run was carried out to simulate the 1950–2015 historical period. The model state on the last day of the year 2015 was taken as the central state for the ensemble. An ensemble of perturbations created with the second-order exact sampling method (Pham et al., 1998) was added to the ocean part of this central state to generate the initial ensemble for the ocean component (see Supporting Information S1). The atmosphere part of the central state was directly used as the initial state for all ensemble members in the atmosphere. The atmosphere ensemble spread attains a quasiequilibrium within one month of the simulation period due to chaotic error growth in the atmosphere induced by the ocean states. Thereafter, the atmosphere states resemble largely uncorrelated weather patterns across the ensemble.

SCDA has the same model setup as WCDA. The only difference is the DA configuration. In SCDA, the atmosphere variables are jointly updated by DA together with the ocean variables through the cross covariances between the two components, while WCDA only updates the ocean variables. The updated variables in the atmosphere are air temperature, surface pressure, vorticity, divergence, and humidity. In the atmosphere, a localization radius of 300 km is set in the horizontal direction, which is the same as used in the ocean to ensure consistency. In one SCDA setup (SCDA), no vertical localization is implemented in the atmosphere. In a second SCDA setup (SCDA_vert), the full DA increment is applied for all atmosphere variables from the surface to 800 hPa pressure level; between 800and 600 hPa the DA increment is linearly decreased from full increment to zero at 600 hPa; above 600 hPa there is no update by assimilation at all.

Besides the assimilation runs, free-run simulations without DA are also performed for comparison purposes. A summary of the simulation scenarios is given below:

1. Free_run: Free-run simulations without DA;

2. WCDA: WCDA run updating only ocean variables;
3. SCDA: SCDA run updating both ocean and atmosphere variables, without vertical localization for atmosphere;
4. SCDA_vert: SCDA run updating both ocean and atmosphere variables with vertical localization for atmosphere.

The performance evaluation measure is the RMSE of ocean and atmosphere variables to quantify the difference between model simulations (the 24 hr-forecasts that serve as the model background in the DA) and observations/reanalysis data:

$$\mathrm{RMSE}(X) = \sqrt{\frac{\sum_{i=1}^{n_t} \sum_{j=1}^{n_{\mathrm{obs}}} \left[\left(\bar{X}_{i,j}^{\mathrm{sim}} - \bar{X}_{i,j}^{\mathrm{obs}}\right) a_j\right]^2}{\sum_{i=1}^{n_t} \sum_{j=1}^{n_{\mathrm{obs}}} {a_j}^2}} \tag{3}$$

where X can be SST, subsurface temperature or salinity for the ocean, and air temperature or wind velocity in the atmosphere; n_t is the number of time steps, n_{obs} the total number of observations/reanalysis data points, which varies for different analysis steps; a_j is the area of the grid cell j. The overbar indicates ensemble average, the superscript *sim* refers to the model simulations at a certain time step before data assimilation and the superscript *obs* the observations at the same time step.

4. Results and Discussion

The four different scenarios described previously are analyzed and discussed in this section. First, results are evaluated for the ocean. The RMSE for SST was calculated by comparing the model forecast with the SST observations used for the DA experiments. In contrast, the RMSE for the subsurface temperature and salinity was calculated by comparing the simulation with the independent EN4 profile data from the UK Met Office (Good et al., 2013). From the RMSE values, we also calculated the relative error, which expresses the improvement compared to the free-run:

$$R(X) = \frac{\mathrm{RMSE}_{\mathrm{scenario}}(X)}{\mathrm{RMSE}_{\mathrm{free}}(X)} \tag{4}$$

Compared to the free-run, both WCDA and SCDA improve the forecast of the temperature. The reduction for RMSE of SST is 64%, 61%, and 64% for WCDA, SCDA, and SCDA_vert, respectively. The SCDA run without vertical localization gives slightly larger RMSE(*SST*) than the WCDA run, while the vertically localized SCDA simulation gives the same RMSE(*SST*) as the WCDA run. The three assimilation runs lead to similar results for the subsurface temperature with an RMSE reduction of 20% for WCDA run and 19% for two SCDA runs. The improvement for salinity is relatively limited and the RMSE is only reduced by 5% for WCDA run, 3% for SCDA, and 4% for SCDA_vert.

The two SCDA runs give similar bias (average SST difference between the model simulation and the observations over 10 months) maps to the WCDA run, see Figure S1 and Tang et al. (2020). As SCDA directly updates the atmosphere variables, the following discussion will concentrate on the performance of different DA runs on the atmosphere component.

In general, the global area-weighted annual average 2 m-temperature bias is −0.17°C for the free run, +0.43°C for WCDA, +0.45°C for SCDA, and +0.43°C for SCDA_vert. Compared to the free run, DA slightly warms up the atmosphere almost everywhere in the ocean (Figures 1a–1d) while the SST difference does not show such general bias as the 2 m-temperature (Figure S6). Over the ocean, DA leads to a small rather uniform warm bias everywhere except for a negative bias in the Arctic. Over the continents there are warm and cold biases. WCDA reduces the warm bias around the west coast of South Africa and northern Pacific. However, this reduction is smaller in case of SCDA, see Figure 1e. Over Europe, Asia, and North and South America the amplitude of the bias is mainly reduced in SCDA compared to WCDA, while it is increased over the tropical South America and parts of Antarctica. Further, the amount of bias is slightly increased over Australia. Generally, while differences between SCDA and WCDA are only moderate (Figure 1e), differences between SCDA_vert and WCDA are even much smaller (Figure 1f). Thus, the larger effects visible in SCDA are caused by the changes in the free atmosphere, which dynamically feed back to the planetary boundary layer.

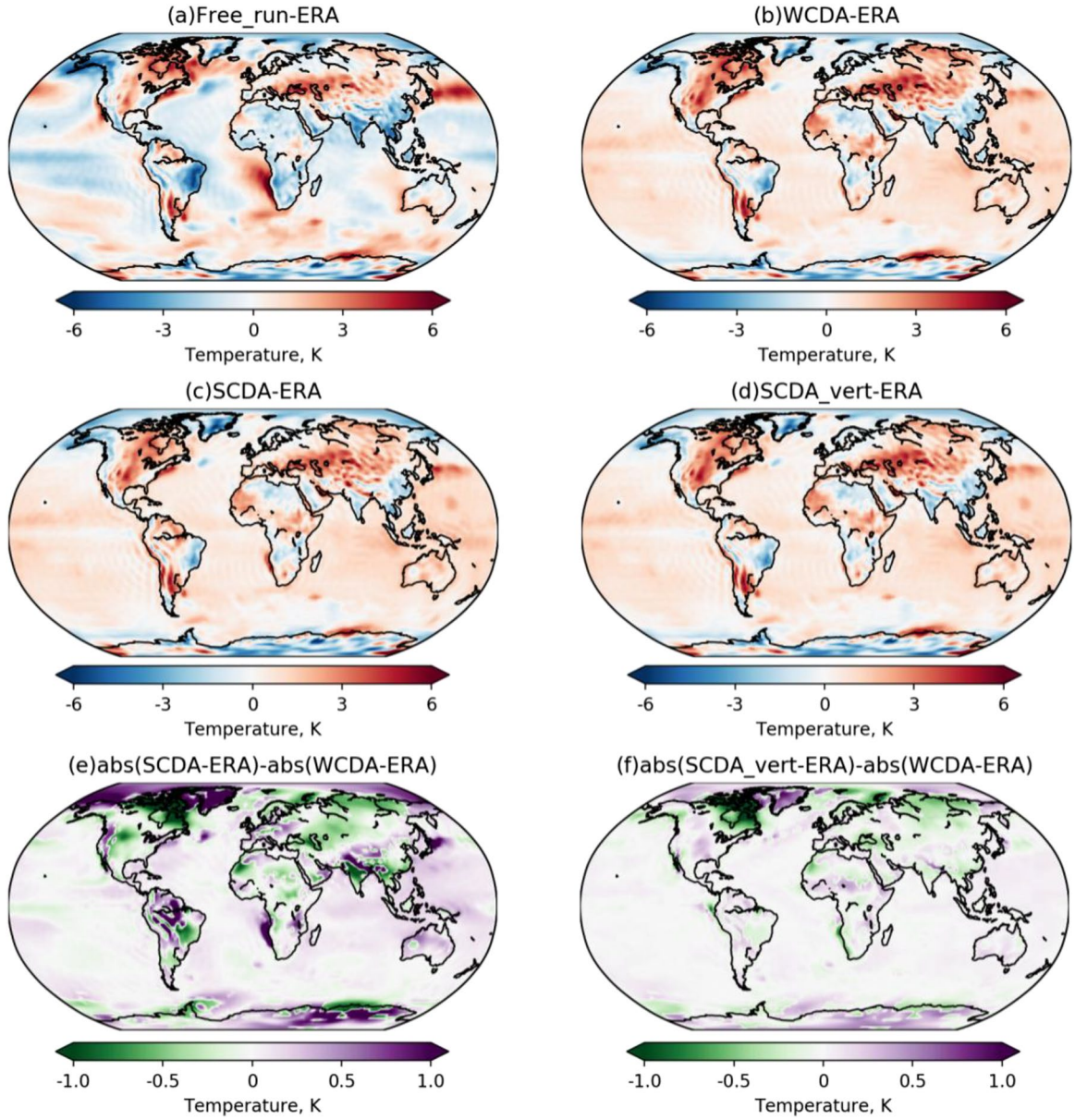

Figure 1. (a–d) Average bias (model simulation - ERA-interim) of temperature at 2 m above surface for the free run and assimilation runs; (e and f) average difference of the absolute bias of 2 m temperature between two strongly coupled data assimilation (SCDA) runs and weakly coupled data assimilation (WCDA) run. Values are averaged over months March–December.

Regarding the wind speed at 10 m height, compared to the free run, both the positive and negative biases along the Equator in the Pacific Ocean and the Atlantic Ocean are strongly reduced by WCDA (Figure 2b) and SCDA (Figures 2c and 2d). The bias reduction by SCDA is weaker than by WCDA, shown in Figure 2e. WCDA also reduces the bias in the Southern and Northern Pacific, which is not the case for SCDA. The positive bias is strengthened by WCDA in the Southern Indian Ocean, and this is even stronger by SCDA. Both WCDA and SCDA introduce positive bias in the Southern Ocean, south of Africa, where the free run shows negative bias. Again, when vertical localization is used in SCDA_vert, the DA effect is more similar to that of WCDA.

Note that the vertical localization can have no direct effect on the 2 m-temperature and the 10 m-wind speed. However, there is also the effect of the model dynamics. The effect is here that without vertical localization also the atmosphere above the boundary layer is modified by the assimilation. These changes will then influence the

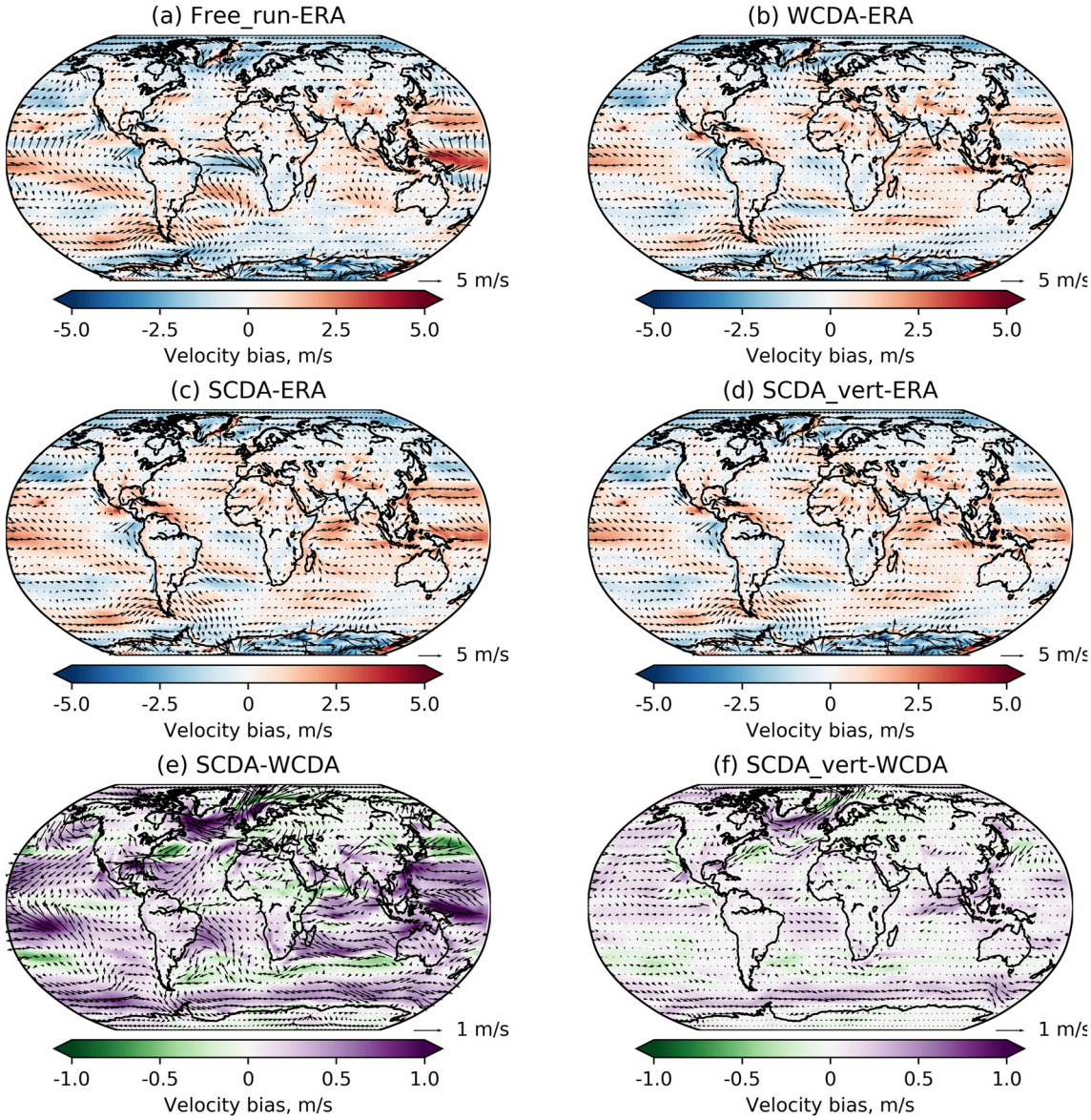

Figure 2. (a–d) Average bias (model simulation – ERA-interim) of wind speed at 10 m above surface for the free run and assimilation runs; (e and f) average difference of 10 m wind speed between the two strongly coupled data assimilation (SCDA) runs and weakly coupled data assimilation (WCDA) run. Values are averaged over months March–December.

lower atmosphere through the dynamics. Since during the assimilation process the daily assimilation updates and the 1-day forecasts alternate we only see the combined effect.

Figure 3 shows the zonal mean RMSE of the atmosphere temperature, wind speed and specific humidity at different pressure levels. Between 650and 1000 hPa, that is, in the lower half of the troposphere, the zonal mean RMSE of temperature (RMSE(T)) is reduced almost everywhere by DA compared to the free run. This is especially the case in the tropics and lower latitudes between 30°N and 30°S (Figure 3b). Between 900 hPa and 500 hPa the RMSE(T) is slightly increased by WCDA in the Arctic (Figure 3b), while the two SCDA runs reduce it (Figures 3c and 3d). However, DA increases the RMSE(T) close to the equator between 10°N and 10°S in the height range between 650and 450 hPa, independent of whether WCDA or SCDA is applied. This is mainly caused by an amplification of the near-surface warming (Figure 1b) with increasing height due to the temperature dependence of the moist adiabatic lapse rate, which leads to a pronounced warm bias in the upper tropical troposphere in the DA runs (see Figure S4). Compared to WCDA, SCDA yields up to 0.5 K larger RMSE(T) between 25°N and 25°S

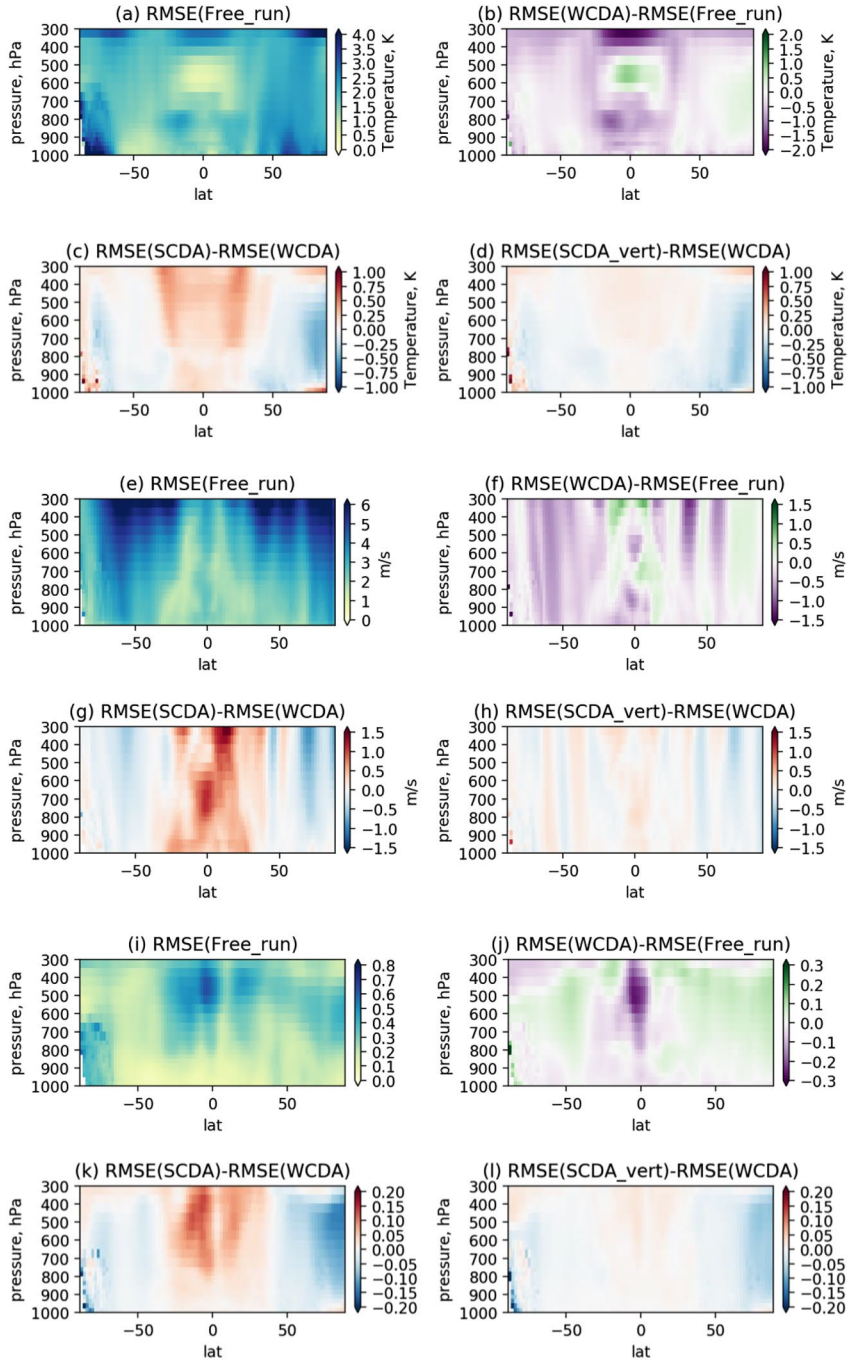

Figure 3. (a) Zonal mean root mean square error (RMSE) of temperature as a function of pressure for Free_run; (b) RMSE difference of temperature between weakly coupled data assimilation (WCDA) and Free_run; (c and d) RMSE difference of temperature between strongly coupled data assimilation (SCDA) and WCDA; (e) zonal mean RMSE of wind speed for Free_run; (f) RMSE difference of wind speed between WCDA and Free_run, (g and h) RMSE difference of wind speed between SCDA and WCDA; (i) normalized zonal mean RMSE of specific humidity for Free_run, (j) normalized zonal mean RMSE difference of specific humidity between WCDA and Free_run, (k and l) normalized zonal mean RMSE difference of specific humidity between SCDA and WCDA. RMSEs of specific humidity were normalized with the ERA-interim specific humidity to account for the strong humidity gradients (in particular in the vertical).

but smaller RMSE(T) in the high-latitude regions. The difference for SCDA_vert (Figure 3d) shows again that the increased errors are caused mainly by the changes of the atmosphere variables introduced by DA in the free atmosphere. Accordingly, the difference between SCDA_vert and WCDA is again minor, except for the notable error reduction in the Arctic troposphere. Here, the improvement is apparently induced in the lower atmosphere and the model dynamics convey the improvement into the upper troposphere. The vertically localized SCDA exerts stronger additional influence in the Arctic compared to other latitudes. Possible reasons include the presence of sea ice (suppressing SST variations and their influence on the atmosphere) and the shallowness of the Arctic boundary layer. This implies that the localization profile covers a larger part of the free atmosphere in the Arctic compared to lower latitudes. Since there are no SST observations north of 80°N, the effects in the Arctic are purely dynamic. The assimilation also influences the winds at different levels in the atmosphere. Between 800 hPa and the ground level, the zonal mean RMSE of horizontal wind speed (RMSE(ws)) in the equatorial region is reduced by WCDA and SCDA_vert (Figures 3f and 3h). SCDA gives almost the same RMSE(ws) as the free run in this region (Figure 3g). Thus, the changes in the free atmosphere feed back to the circulation in the lower atmosphere. Slightly increased RMSE(ws) is observed north of the equator between 800 hPa and 600 hPa, the region between 20°N and 20°S above 500 hPa and the northern high latitude regions above 800 hPa in WCDA. For the rest of the regions WCDA reduces the RMSE(ws). In general, SCDA shows larger RMSE(ws) between 25°N and 25°S than the free run and WCDA from ground to the free atmosphere up to 300 hPa, but outside of the tropical region the velocity is improved compared to the free run (Figure 3g). SCDA_vert gives similar results as WCDA (Figure 3h). This suggests again that the direct DA increments in the lower troposphere do not add much to the changes communicated from the DA-corrected ocean surface state to the atmosphere through the coupling, whereas direct increments in the higher troposphere exert a stronger additional influence.

A further effect of the assimilation is visible in the specific humidity. Large normalized RMSEs (RMSE(q)) are visible in the free run (Figure 3i) in the tropics at heights above 800 hPa, south of 70°S between 650 hPa and the ground, and north of 60°N between 800 and 400 hPa. The RMSE(q) along the equator, especially in the higher atmosphere above 600 hPa, is largely reduced (Figure 3j) because the corrected equatorial SSTs (reduced cold bias) generate stronger ascending motion and transport more moisture into the upper troposphere (see Tang et al., 2020). This effect is particularly strong for WCDA (Figure 3j) and SCDA_vert (Figure 3l), but smaller for SCDA with updates throughout the atmosphere. Slightly smaller RMSE(q) is found in the southern hemisphere north of 40°S for WCDA compared to the free run, while the RMSE in this region is slightly larger for SCDA than the free run. Like for the temperature in Figures 3a–3d, WCDA slightly deteriorates the state in the Arctic, while SCDA improves it. Similar to temperature and wind velocity, the humidity difference between SCDA_vert and WCDA is mostly minor, except for the Arctic where a smaller RMSE(q) is obtained for SCDA_vert.

From WCDA experiments discussed by Tang et al. (2020) we already know that assimilating only SST has a substantial effect on tropical and subtropical temperature profiles in the atmosphere. The lower atmosphere responds quickly to the changed SST even if it is not constrained directly by the DA. In case of SCDA, the atmosphere is directly influenced and then reacts also dynamically. However, this combination only leads to a small additional effect of slightly higher temperatures in the lower atmosphere.

WCDA corrects the cold bias of the lower atmosphere only in the tropics but not in the high latitudes. In contrast, the two SCDA experiments can improve the bias in the Arctic. This positive effect not only holds for the air temperature but also for other atmosphere variables like the wind speed and the specific humidity. This indicates that SCDA_vert can preserve the good performance of WCDA in the tropics and subtropics. At the same time it can improve the atmosphere simulation in the high latitudes which benefits from SCDA, possibly linked with the presence of sea ice (suppressing SST variations) and the shallow boundary layer. However, both of them deteriorate the simulation of atmosphere temperatures corrected by SST observations through coupling.

5. Conclusions

In this paper, SCDA is applied for a global coupled ocean-atmosphere model. By assimilating satellite SST observations, we explore the influence of SCDA on the ocean and the atmosphere. The ocean and the atmosphere variables are simultaneously updated by the LESTKF utilizing the cross-covariances between the SST and the atmosphere variables. Results are compared with our previous WCDA experiment, where only the ocean variables are directly updated by DA. SCDA of SST observations yield a similar performance in simulating the ocean

as WCDA. For the atmosphere, SCDA gives overall slightly worse results than WCDA if no vertical localization is applied. With vertical localization in the atmosphere that constrains DA increments to the lower troposphere, the difference between SCDA and WCDA is quite minor. An exception is the Arctic region, where SCDA, with and without vertical localization, improves the atmosphere. This suggests that the improvements in the Arctic are due to improvements in the lower atmosphere, which are dynamically transported to higher levels. The weak effect of SCDA with vertical localization compared to WCDA in the tropical to midlatitude regions implies that the SSTs already exert a strong influence on the lower troposphere. This implies SCDA should only be done with vertical localization in order to avoid changes in the higher atmosphere due to the unrealistic ensemble-estimated covariances, which then feed back dynamically to the planetary boundary layer.

In contrast to SCDA studies that assimilate atmosphere observations and update ocean variables via the covariances, which show a clear benefit in the ocean from the atmosphere observations, we found rather moderate improvements of the atmosphere caused by SCDA of ocean observations compared to WCDA. This asymmetry is likely linked to the different time scales in the atmosphere and the ocean. In our experiments, the slower ocean SST is used to update the faster atmosphere. Nevertheless, the experiments show that there can be positive effects, in particular in the Arctic region.

A related limitation of our study is that, in contrast to numerical weather prediction systems, the atmosphere is unconstrained, except for the influence exerted by the SST and, in case of the SCDA, the cross-compartment DA increments. Thus, the different DA ensemble members exhibit largely independent random weather states rather than states that sample only uncertainty around the state of the observed real atmosphere. Consequently, the influence of the SST-DA on the atmosphere can largely be linked to impacts on the mean state rather than how the evolution of weather-related variability is captured. Similar studies with a directly constrained atmosphere could explore to what degree the SCDA of ocean observations can help further constrain the atmospheric state when the atmosphere is already more strongly constrained in the first place.

In the experiments performed here, the instantaneous covariances between SST and the atmosphere variables were utilized for SCDA. To filter out the fastest dynamics of the atmosphere, one could envision to use the covariances between the instantaneous ocean state and averaged atmosphere fields, for example, over one day. However, initial experiments of this approach were not successful. Further work should be aimed in this direction to make the observations of the ocean more useful for atmosphere-ocean SCDA.

Data Availability Statement

Open Research: The AWI climate model AWI-CM version 1.1 used for this research can be accessed from the esm-tool at Zenodo (Barbi et al., 2020). PDAF is available from the website http://pdaf.awi.de, after registration. The observation data used in this study can be downloaded from the Copernicus website https://resources.marine.copernicus.eu/?option=com_csw&view=details&product_id=SST_GLO_SST_L3S_NRT_OBSERVATIONS_010_010, and the UK MetOffice website https://www.metoffice.gov.uk/hadobs/en4/download-en4-2-1.html. The ERA-interim reanalysis data can be downloaded from the ECMWF website https://apps.ecmwf.int/datasets/data/interim-full-daily/. The input data for the numerical modeling can be found in Rackow et al. (2019). The output data for the numerical experiments related to this article can be found at Zenodo https://doi.org/10.5281/zenodo.5717555 (Tang et al., 2021).

Acknowledgments
The work described in this paper has received funding from the Initiative and Networking Fund of the Helmholtz Association through the project "ESM - Advanced Earth System Modelling Capacity." The authors acknowledge the North-German Supercomputing Alliance (HLRN) for providing HPC resources in the project hbk00064. The authors gratefully acknowledge the Earth System Modelling Project (ESM) for funding this work by providing computing time on the ESM partition of the supercomputer JUWELS (Jülich Supercomputing Centre, 2019) at the Jülich Supercomputing Centre (JSC). H. F. G. and L. M. acknowledge the financial support by the Federal Ministry of Education and Research of Germany in the framework of SSIP (grant 01LN1701A). Open access funding enabled and organized by Projekt DEAL.

References

Barbi, D., Gierz, P., Wieters, N., Cristini, L., Streffing, J., Andrés-Martinez, M., et al. (2020). *esm-tools/esm_tools: Release 4 (Version v4.0.3)*. Zenodo. https://doi.org/10.5281/zenodo.3797121

Browne, P. A., de Rosnay, P., Zuo, H., Bennett, A., & Dawson, A. (2019). Weakly coupled ocean–atmosphere data assimilation in the ECMWF NWP system. *Remote Sensing*, *11*(3), 234. https://doi.org/10.3390/rs11030234

Good, S. A., Martin, M. J., & Rayner, N. A. (2013). EN4: Quality controlled ocean temperature and salinity profiles and monthly objective analyses with uncertainty estimates. *Journal of Geophysical Research*, *118*(12), 6704–6716. https://doi.org/10.1002/2013JC009067

Han, G., Wu, X., Zhang, S., Liu, Z., & Li, W. (2013). Error covariance estimation for coupled data assimilation using a Lorenz atmosphere and a simple pycnocline ocean model. *Journal of Climate*, *26*(24), 10218–10231. https://doi.org/10.1175/JCLI-D-13-00236.1

Jülich Supercomputing Centre. (2019). JUWELS: Modular Tier-0/1 supercomputer at the Jülich supercomputing centre. *Journal of Large-Scale Research Facilities*, *5*, A135. https://doi.org/10.17815/jlsrf-5-171

Karspeck, A. R., Danabasoglu, G., Anderson, J., Karol, S., Collins, N., Vertenstein, M., et al. (2018). A global coupled ensemble data assimilation system using the community earth system model and the data assimilation research testbed. *Quarterly Journal of the Royal Meteorological Society*, *144*(717), 2404–2430. https://doi.org/10.1002/qj.3308

Kunii, M., Ito, K., & Wada, A. (2017). Preliminary test of a data assimilation system with a regional high-resolution atmosphere-ocean coupled model based on an ensemble Kalman filter. *Monthly Weather Review*, *145*(2), 565–581. https://doi.org/10.1175/mwr-d-16-0068.1

Laloyaux, P., Balmaseda, M., Dee, D., Mogensen, K., & Janssen, P. (2016). A coupled data assimilation system for climate reanalysis. *Quarterly Journal of the Royal Meteorological Society*, *142*(694), 65–78. https://doi.org/10.1002/qj.2629

Mu, L., Nerger, L., Tang, Q., Loza, S. N., Sidorenko, D., Wang, Q., et al. (2020). Toward a data assimilation system for seamless sea ice prediction based on the AWI climate model. *Journal of Advances in Modeling Earth Systems*, *12*(4), e2019MS001937. https://doi.org/10.1029/2019MS001937

Mulholland, D. P., Laloyaux, P., Haines, K., & Balmaseda, M. A. (2015). Origin and impact of initialization shocks in coupled atmosphere–ocean forecasts. *Monthly Weather Review*, *143*(11), 4631–4644. https://doi.org/10.1175/MWR-D-15-0076.1

Nerger, L., & Hiller, W. (2013). Software for ensemble-based data assimilation systems—Implementation strategies and scalability. *Computers & Geosciences*, *55*, 110–118. https://doi.org/10.1016/j.cageo.2012.03.026

Nerger, L., Hiller, W., & Schröter, J. (2005). PDAF-the parallel data assimilation framework: Experiences with Kalman filtering. In *Use of high performance computing in meteorology* (pp. 63–83). World Scientific. https://doi.org/10.1142/9789812701831_0006

Nerger, L., Janjić, T., Schröter, J., & Hiller, W. (2012a). A regulated localization scheme for ensemble-based Kalman filters. *Quarterly Journal of the Royal Meteorological Society*, *138*(664), 802–812. https://doi.org/10.1002/qj.945

Nerger, L., Janjić, T., Schröter, J., & Hiller, W. (2012b). A unification of ensemble square root Kalman filters. *Monthly Weather Review*, *140*(7), 2335–2345. https://doi.org/10.1175/MWR-D-11-00102.1

Nerger, L., Tang, Q., & Mu, L. (2020). Efficient ensemble data assimilation for coupled models with the parallel data assimilation framework: Example of AWI-CM (AWI-CM-PDAF 1.0). *Geoscientific Model Development*, *13*(9), 4305–4321. https://doi.org/10.5194/gmd-13-4305-2020

Penny, S. G., Bach, E., Bhargava, K., Chang, C.-C., Da, C., Sun, L., & Yoshida, T. (2019). Strongly coupled data assimilation in multiscale media: Experiments using a quasi-geostrophic coupled model. *Journal of Advances in Modeling Earth Systems*, *11*(6), 1803–1829. https://doi.org/10.1029/2019MS001652

Penny, S. G., & Hamill, T. M. (2017). Coupled data assimilation for integrated earth system analysis and prediction. *Bulletin of the American Meteorological Society*, *98*(7), ES169–ES172. https://doi.org/10.1175/BAMS-D-17-0036.1

Pham, D. T., Verron, J., & Roubaud, M. C. (1998). A singular evolutive extended Kalman filter for data assimilation in oceanography. *Journal of Marine Systems*, *16*(3–4), 323–340. https://doi.org/10.1016/S0924-7963(97)00109-7

Rackow, T., Goessling, H. F., Jung, T., Sidorenko, D., Semmler, T., Barbi, D., & Handorf, D. (2018). Towards multi-resolution global climate modeling with ECHAM6-FESOM. Part II: Climate variability. *Climate Dynamics*, *50*(7), 2369–2394. https://doi.org/10.1007/s00382-016-3192-6

Rackow, T., Sein, D. V., Semmler, T., Danilov, S., Koldunov, N. V., Sidorenko, D., et al. (2019). Sensitivity of deep ocean biases to horizontal resolution in prototype CMIP6 simulations with AWI-CM1. 0. *Geoscientific Model Development*, *12*(7), 2635–2656. https://doi.org/10.5194/gmd-12-2635-2019

Sidorenko, D., Rackow, T., Jung, T., Semmler, T., Barbi, D., Danilov, S., et al. (2015). Towards multi-resolution global climate modeling with ECHAM6–FESOM. Part I: Model formulation and mean climate. *Climate Dynamics*, *44*(3–4), 757–780. https://doi.org/10.1007/s00382-014-2290-6

Sluka, T. C., Penny, S. G., Kalnay, E., & Miyoshi, T. (2016). Assimilating atmospheric observations into the ocean using strongly coupled ensemble data assimilation. *Geophysical Research Letters*, *43*(2), 752–759. https://doi.org/10.1002/2015gl067238

Smith, P. J., Fowler, A. M., & Lawless, A. S. (2015). Exploring strategies for coupled 4D-Var data assimilation using an idealised atmosphere-ocean model. *Tellus A: Dynamic Meteorology and Oceanography*, *67*(1), 27025. https://doi.org/10.3402/tellusa.v67.27025

Stevens, B., Giorgetta, M., Esch, M., Mauritsen, T., Crueger, T., Rast, S., et al. (2013). Atmospheric component of the MPI-M earth system model: ECHAM6. *Journal of Advances in Modeling Earth Systems*, *5*(2), 146–172. https://doi.org/10.1002/jame.20015

Tang, Q., Mu, L., Goessling, H., Semmler, T., & Nerger, L. (2021). *Data for the article entitled "Strongly coupled data assimilation of ocean observations into an ocean-atmosphere model" by Tang et al. 2021, GRL [Data set]*. Zenodo. https://doi.org/10.5281/zenodo.5717555

Tang, Q., Mu, L., Sidorenko, D., Goessling, H., Semmler, T., & Nerger, L. (2020). Improving the ocean and atmosphere in a coupled ocean-atmosphere model by assimilating satellite sea-surface temperature and subsurface profile data. *Quarterly Journal of the Royal Meteorological Society*, *146*, 4014–4029. https://doi.org/10.1002/qj.3885

Tardif, R., Hakim, G. J., & Snyder, C. (2014). Coupled atmosphere-ocean data assimilation experiments with a low-order climate model. *Climate Dynamics*, *43*(5), 1631–1643. https://doi.org/10.1007/s00382-013-1989-0

Valcke, S., Craig, T., & Coquart, L. (2013). *OASIS3-MCT user guide, OASIS3-MCT 2.0, 1875*. CERFACS/CNRS SUC URA. Retrieved from https://oasis.cerfacs.fr/wp-content/uploads/sites/114/2021/02/GLOBC-Valcke_TR_OASIS3-MCT_2.0_2013.pdf

Wang, Q., Danilov, S., Sidorenko, D., Timmermann, R., Wekerle, C., Wang, X., et al. (2014). The finite element sea ice-ocean model (FESOM) v.1.4: Formulation of an ocean general circulation model. *Geoscientific Model Development*, *7*(2), 663–693. https://doi.org/10.5194/gmd-7-663-2014

Zhang, S., Liu, Z., Zhang, X., Wu, X., Han, G., Zhao, Y., et al. (2020). Coupled data assimilation and parameter estimation in coupled ocean–atmosphere models: A review. *Climate Dynamics*, *54*, 5127–5144. https://doi.org/10.1007/s00382-020-05275-6

Zhang, Z., & Moore, J. C. (2015). Chapter 9: Data Assimilation. In Z. Zhang, & J. C. Moore (Eds.), *Mathematical and physical fundamentals of climate change* (pp. 291–311). Elsevier. https://doi.org/10.1016/B978-0-12-800066-3.00009-7